Design of Passivity Based Robust Control of AC / DC Power Converter for Power Factor Improvement and Voltage Regulation

[1]K.Udhayakumar, [2]P. Lakshmi, and [3]M. Sudalaimani

[1]Lecturer, [2]Assistant Professor and [3]Post Graduate Scholar
Department of Electrical and Electronics Engineering,
College of Engineering Guindy, Anna University, Chennai 600 025, India
[[1]Communicating Author, Email: k_udhayakumar@annauniv.edu]

Abstract:

In this work an Interconnection-and-Damping Assignment Passivity-based control (IDA-PBC) for a full-bridge rectifier is investigated. The controller design takes advantage of the generalized state space averaging (GSSA) modeling technique to convert the quoted nonstandard problem (in actual variables) into a standard regulation one (in GSSA variables). The transient behavior of the system, along with the controller is obtained through computer simulation. The closed-loop system performance fulfils unity power factor in the AC mains and output DC voltage regulation. In particular, the technique is shown to be effective and robust with respect to load variations.

Key terms: Passivity Based Control, Generalized State Space Averaging (GSSA), AC-DC power converter.

1. INTRODUCTION

In recent years, single-phase switch-mode AC/DC power converters have been increasingly used in the industrial, commercial, residential, aerospace, and military environment. To get constant output voltage and near unity power factor, it is essential that the converter has to be controlled [1]. In recent power electronic researches, high power density, high power factor, high efficiency, low current distortion, and simple control scheme are strongly recommended for the industrial applications [2]. This is due to the enforcement of strict harmonic regulations such as IEC 1000-3-2. Voltage source converters provide excellent control over power flow in both directions. They can be operated as AC–DC converters to generate regulated DC voltage at high input

power factor. The power flow can easily be reversed to operate the converter as a DC–AC converter [3]. This capability makes the system ideally suited to electric drives and line interactive UPS applications. Conventional diode rectifiers or phase-controlled rectifiers have properties of simple structure and low cost. However, they have the inherent drawbacks that the power factor decreases when the firing angle increases and the line current harmonics are relatively high. To overcome the above problems, several circuit topologies of the single-phase switching mode rectifier (SMR) with low current distortion and unity power factor have been proposed in the past few years [4]. These circuit configurations are based on the full bridge diode rectifier followed by a boost, buck boost, or cuk converter. Single-phase full bridge and half bridge SMR circuit configurations have capabilities of bidirectional power flow, reactive power control, and high power factor.

Among these circuit topologies, single-phase unidirectional AC/DC converters with boost topology have been widely used as front-end power factor pre-regulator due to its good performance characteristics. The boost topology has properties of high power factor, low current distortion, step-up voltage ratio and continuous input current. Boost rectifier topologies can be broadly classified as continuous mode and discontinuous mode conduction rectifiers [5]. The single-phase two-level PWM continuous current mode rectifier with unidirectional power flow is presented here.

The generalized state-space averaging method is a way to model the power converters as time independent systems, defined by unified set of differential equations, capable of representing circuit waveforms without discontinuities [6]. Consequently, this approach is not suitable for modeling converters which have dominant oscillatory behavior such as the resonant type converters or large ripple PWM converters [7]. Therefore, analysis of AC/DC power converters with ideal switches and parasitic components (capacitors of inductors) forming loops must be considered with more care. With the generalized state-space averaging method, the circuit state variables are approximated by a Fourier series expansion with time-dependent coefficients [8]. This representation results in an unified time-invariant set of differential

equations where the state variables are the coefficients of the corresponding Fourier series of the circuit variables.

The paper is organized as follows. Section 2 studies the dynamics of a single-phase full-bridge boost converter circuit and develops a state space model. In section 3, the converter model is analyzed in the frame of Port-Controlled Hamiltonian System (PCHS) form. Section 4 presents the controller design based on IDA-PB control technique. The simulation results are shown in section 5 for the robustness and effectiveness of the technique employed. Finally some concluding remarks are drawn.

2. PROPOSED BOOST RECTIFIER

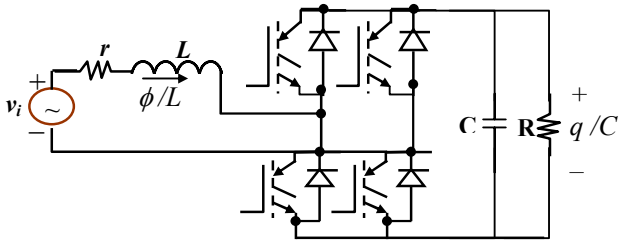

Figure 1 Single phase Full-bridge Boost Rectifier

Figure 1 shows the single phase full-bridge boost rectifier. The transistor works as a switch, which is turned on and off by the PWM control signal.

2.1 State Space Modeling:

The system behaviour is obtained by solving the modelling equations. Mathematical modelling also decides the details of the system that can possibly be studied by computer simulation. The starting point for modelling a converter, however, is by application of Kirchoff's and Ohm's law to the circuit, which provides first-order differential equations describing the state of current through inductor(s) and voltage across capacitor(s).

The following equations describe the dynamical behaviour of the full-bridge boost type rectifier in Figure 1.

$$\begin{aligned}\frac{d\phi(t)}{dt} &= \frac{-u(t)}{C}q(t) - \frac{r}{L}\phi(t) + V_i(t)\\ \frac{dq(t)}{dt} &= \frac{u(t)}{L}\phi(t) - i_l(t)\end{aligned} \tag{2.1}$$

where $\phi(t)$ is the magnetic flux through inductor, $q(t)$ is the electrical charge in capacitor , r is a resistance modelling the parasitic resistive effect of the inductor and the switches, u(t) describes the position of the switches taking values in the discrete set , $i_l(t)$ is the load current, and $V_i(t)$=E sin(ω_ot) is the AC voltage source of amplitude and angular frequency $\omega_o=2\pi f$, f being the frequency in Hertz.

In this section, and for GSSA modelling purposes, the load will be assumed resistive, then $i_l(t)=q(t)$/RC.

A useful variable transformation, which simplifies (2.1), forthcoming developments, is obtained through v(t)= -u(t)q(t) and z = [z_1 z_2] = [$\phi(t)$, (1/2)q(t)^2] . The system in the new variables is,

$$\frac{dz_1(t)}{dt} = \frac{-rz_1(t)}{L} + \frac{v(t)}{C} + v_i(t) \tag{2.2}$$

$$\frac{dz_2(t)}{dt} = \frac{-v(t)z_1(t)}{L} - i_l(t)\sqrt{2z_2(t)} \tag{2.3}$$

The energy in the storing elements and of this system can be described by,

$$H_T(t) = \frac{z_1(t)^2}{2L} + \frac{z_2(t)}{C} \tag{2.4}$$

And (2.2) & (2.3) can be rewritten as

$$\begin{bmatrix}\frac{dz_1(t)}{dt}\\ \frac{dz_2(t)}{dt}\end{bmatrix} = \begin{bmatrix}0 & v\\ -v & 0\end{bmatrix}\frac{\partial H_T}{\partial z} - \begin{bmatrix}r & 0\\ 0 & Ci_l\sqrt{2z_2}\end{bmatrix}\frac{\partial H_T}{\partial z} + \begin{bmatrix}v_i\\ 0\end{bmatrix} \tag{2.5}$$

This corresponds to a PCHS system of the form,

$$\dot{z} = [J_T(v) - R_T(x)]\frac{\partial H_T}{\partial z}(z) + g_T \tag{2.6}$$

Where $J_T = -J_T^T$, $R(x) = R^T(x) \geq 0$ are the matrices describing the interconnection structure and damping, respectively. The last inequality results from and because

the load voltage is non negative. The input voltage is considered as an external disturbance modelled by vector. In order to obtain the simplest coherent GSSA model, let us determine the harmonic content of the states and the input in steady state.

2.3 Steady State Analysis

To this end, let $z_1^*(t) = LI_d \sin(\omega_0 t)$ be the desired dynamics and $i_l(t)$ be the load current assuming a resistive load. In order to obtain the steady-state zero dynamics, let us take into account this assumption in (2.5) – (2.6) and let us solve for v and z_2. The steady-state response yields,

$$z_2^*(t) = \alpha_{z2} + \beta_{z2} \sin(2\omega_0 t + \theta_{z2}) \tag{2.7}$$

$$v^*(t) = C(E - rI_d)\sin(\omega_0 t) + I_d \omega_0 LC \cos(\omega_0 t) \tag{2.8}$$

Where,

$$\alpha_{z2} = \frac{I_d RC^2}{4}(E - rI_d);$$

$$\beta_{z2} = \frac{I_d RC^2}{4}\sqrt{\frac{(E - rI_d)^2 + (I_d \omega_0 L)^2}{1 + (\omega_0 RC)^2}}$$

$$\tan(\theta_{z2}) = \frac{(E - rI_d) - \omega_0 RC(I_d \omega_0 L)}{\omega_0 RC((E - rI_d) + (I_d \omega_0 L)}$$

The value of parameter I_d can be obtained through power balance.

$$I_d = \frac{E}{2r} \mp \sqrt{\left(\frac{E}{2r}\right)^2 - \frac{2V_d^{\,2}}{rR}} \tag{2.9}$$

The minus sign has been chosen since it yields a stable equilibrium point with lower power consumption. The total stored energy in steady-state results in,

$$H_T(t) = \alpha_H + \beta_H \sin(2\omega_0 t + \theta_H) \tag{2.10}$$

Where,

$$\alpha_H = \frac{I_d CR}{4}(E - rI_d) + \frac{LI_d^2}{4}$$

$$\beta_H = \frac{\alpha_H = \frac{I_d CR}{4}(E - rI_d) + \frac{LI_d^2}{4}}{\sqrt{1 + (\omega_o RC)^2}}$$

$$\tan(\theta_H) = \frac{1}{\omega_o RC}$$

Expressions (2.1), (2.7), and (2.8) show that a suitable GSSA model of the system, useful for controller design purposes, should contemplate the first harmonic Fourier components for $z_1(t)$, the zero and second harmonic Fourier components for $z_2(t)$ and the first harmonic Fourier components for v(t). As for the Hamiltonian $H_T(t)$, from (2.10), the DC component and second harmonic should be considered. If, in addition, C is chosen to obtain a low voltage ripple in the capacitor, then β_{z2} and β_H are negligible with respect to α_{z2} and α_H, respectively. Hence, the second harmonic Fourier components of $z_2(t)$ and $H_T(t)$ will not be considered from now on.

3. FULL BRIDGE RECTIFIER AS A PCH SYSTEM IN GSSA VARIABLES

Although the most general GSSA model of a system has infinite dimension, the harmonic contents of signals in steady state can be used to find accurately enough finite dimensional GSSA models. To this aim, using (2.3) and taking into account the Fourier components we have considered as relevant, the bilinear product $v(t)z_1(t)$ in (2.3) can be approximated as,

$$\langle vz_1 \rangle_0 = \sum_{k=-\infty}^{\infty} \langle v \rangle_{-k} \langle z_1 \rangle_k \approx 2(\langle v \rangle_1^R \langle z \rangle_1^R + \langle v \rangle_1^I \langle z_1 \rangle_1^I) \tag{3.1}$$

Furthermore,

$$\langle i_1 q \rangle_0 = \approx 2(\langle i_l \rangle_1^R \langle q \rangle_1^R + \langle q \rangle_1^I \langle i_1 \rangle_1^I) + \langle i_l \rangle_0 \langle q \rangle_0 \tag{3.2}$$

As it has been assumed q (t) has predominantly DC harmonic components, the complex coefficients of order one in (3.1) will be discarded. Hence, using (3.1) and (3.2), the GSSA model of the system defined by (2.3) becomes,

$$\begin{aligned}
\frac{d(z_2)_0}{dt} &= -\langle i_l \rangle_0 \sqrt{2\langle z_2 \rangle_0 -} \quad \frac{2}{L}\langle \upsilon \rangle_1^R \langle z_1 \rangle_1^R - \frac{2}{L}\langle \upsilon \rangle_1^I \langle z_1 \rangle_1^I \\
\frac{d(z_1)_1^R}{dt} &= -\frac{r}{L}\langle z_1 \rangle_1^R + \frac{1}{C}\langle \upsilon \rangle_1^R + \omega_0 \langle z_1 \rangle_1^I \\
\frac{d(z_1)_1^I}{dt} &= -\frac{r}{L}\langle z_l \rangle_1^I + \frac{1}{C}\langle \upsilon \rangle_1^I + \omega_0 \langle z_1 \rangle_1^R - \frac{E}{2}.
\end{aligned} \tag{3.3}$$

Let, x = [$\langle z_2 \rangle_0$, $\langle z_1 \rangle_1^R, \langle z_1 \rangle_1^I$] be the state and u = [$\langle v_1 \rangle_1^R, \langle v_1 \rangle_1^I$] control vectors, respectively, and

$$x^* = [\frac{C^2 V_d^{\,2}}{2}, 0, \frac{-LI_d}{2}] \tag{3.4}$$

be the desired equilibrium.

The original control problem has become a regulation problem in the GSSA domain. For simplicity, let us denote the load current DC component by $I_0 = \langle i_1 \rangle_0$. Then, the system in (3.3) can be written as the PCH system:

$$\begin{bmatrix} \frac{dx_1(t)}{dt} \\ \frac{dx_2(t)}{dt} \\ \frac{dx_3(t)}{dt} \end{bmatrix} = \begin{bmatrix} 0 & -u_1 & -u_2 \\ u_1 & 0 & \frac{\omega_0 L}{2} \\ u_2 & -\frac{\omega_0 L}{2} & 0 \end{bmatrix} \frac{\partial H}{dx} - \begin{bmatrix} CI_0\sqrt{2x_1} & 0 & 0 \\ 0 & \frac{r}{2} & 0 \\ 0 & 0 & \frac{r}{2} \end{bmatrix} \frac{\partial H}{dx} + \begin{bmatrix} 0 \\ 0 \\ \frac{-E}{2} \end{bmatrix} \tag{3. 5}$$

Or in a more compact form,

$$\dot{x} = [J(u) - R(x)]\frac{\partial H}{dx} + g \tag{3.6}$$

where, J(u) and R(x) are the interconnection-and-damping matrices, respectively, and g vector models an external disturbance. Note that H(x) is the DC component of the Hamiltonian in $H_T(z)$in (2.10); i.e.,

$$H(x) = \frac{1}{C}\langle z_2 \rangle_0 + \frac{1}{L}\langle \phi \rangle_1^{R\,2} + \frac{1}{L}\langle \phi \rangle_1^{I\,2} \tag{3. 7}$$

or, $H(x) = \frac{1}{C} x_1 + \frac{1}{L} x_2^2 + \frac{1}{L} x_3^2$ (3. 8)

The GSSA system in (3.6) preserves the PCH structure of the system in (3.6), with the remarkable advantage of a regulation control objective. This allows the IDA passivity based design approach to be methodically used. In this line, an IDA-PB control fulfilling system specifications is designed in the next section. The control law depends on the output voltage DC component and requires measuring the dc output current to guarantee robustness with respect to load variations.

4. CONTROLLER DESIGN

The final objective of the IDA-PBC approach [8] is to design a feedback control u = ß(x), such that the closed-loop dynamics is the PCH reference system.

$$\dot{x} = [J_d(x) - R_d(x)] \frac{\partial H_d}{dx}(x)$$

where, $J_d(x) = -J_d^T(x)$ and $J_d(x) = R_d^T(x) \geq 0$ are targeted interconnection-and-damping matrices, and the new energy function $H_d(x) = H(x) + H_a(x)$ has a strict local minimum at the desired equilibrium.

4.1 Conditions for Stable Equilibrium:

Following [8], we proceed in the standard manner.

(i) Structure preservation.

Given $J_d(x)$ and $R_d(x)$, let $J_a(x)$ and $R_a(x)$ be defined by,

$J_d(x) = J(x, \beta(x)) + J_a(x) = [J(x, \beta(x)) + J_a(x)]^T$

$R_d(x) = R(x) + R_a(x) = [R(x) + R_a(x)]^T$

Then, the desired dynamics is achieved if it is possible to find functions $\beta(x)$ and $k(x) := \partial H_a(x)/\partial x$ satisfying,

$[J(x, \beta(x)) + J_a(x) - (R(x) + R_a(x))]\, k(x) = -[J_a(x) - R_a(x)]\, \partial H_a(x)/\partial x + g.$

(ii) Integrability.

K(x) is the gradient of a scalar function.

That is, $\frac{\partial k_i}{\partial x_j}(x) = \frac{\partial k_j}{\partial x_i}(x)$.

(iii) Equilibrium condition.

$$\frac{\partial H_d}{\partial x}(x^*) = 0$$

If conditions *(i) – (iii)* hold, then x^* is a (locally) stable equilibrium point of the closed-loop system.

Let us particularise the aforementioned procedure for the full bridge boost rectifier controller defining $J_d(x) = J(x, \beta(x))$ and $R_d(x) = R(x)$,

i.e., $J_a(x) = 0$ and.$R_a(x) = 0$

4.2 Structure Preservation

Equation (1) yields,

$$0 = -I_0 C\sqrt{2x_1 k_1} - u_1 k_2 - u_2 k_3 \tag{4.1}$$

$$0 = u_1 k_1 - \frac{r}{2} + \frac{\omega L}{2} k_3 \tag{4.2}$$

$$0 = u_2 k_1 - \frac{\omega L}{2} k_2 + \frac{E}{2} \tag{4.3}$$

Then, from (4.2) – (4.3),

$$u_1 = \frac{-rk_2 + \omega Lk_3}{2k_1}$$

$$u_2 = \frac{\omega Lk_2 + Rk_3 - e}{2k_1} - \tag{4.4}$$

4.3. Integrability

Replacing (4.4) in (4.1) and taking into account that $k(x) = \partial H_a(x)/\partial x$, the following partial differential equation is obtained:

$$2I_0C\sqrt{2x_1}\left(\frac{\partial H_a}{\partial x_1}\right)^2 = -r\left(\frac{\partial H_a}{\partial x_2}\right)^2 - \left(r\frac{\partial H_a}{\partial x_3} - E\right)\frac{\partial H_a}{\partial x_3}$$

As we are interested in control inputs u_1, u_2 , which only depend on the output voltage dc component, we take $k_2 = k_2(x_1)$ and $k_3 = k_3(x_1)$. Then, by the Integrability condition ,

$$\frac{\partial k_i}{\partial x_1} = \frac{\partial^2 H_a}{\partial x_1 \partial x_i} = \frac{\partial^2 H_a}{\partial x_i \partial x_1} = 0$$

for i = 2, 3 and $k_2 = a_2$ and $k_3 = a_3$ are indeed constant. Thus, the PDE is actually an ODE on, whose solution is given by,

$$H_a(x) = -\frac{2}{3}\sqrt{\sqrt{\frac{2x}{I_0C}}x_1(a_2^2r + a_3^2r - a_3E)} + a_2x_2 + a_3x_3 \qquad (4.5)$$

4.4 Equilibrium Assignment

From (4.3) and the definition of H_a , the following conditions on a_2, a_3 and I_d so that x^*, from (4.2), is a singular point of H_d are derived

$$\frac{1}{C} + \frac{\sqrt{-2I_oC\sqrt{C^2V_d^2}(a_2^2r + a_3^2r - a_3E)}}{3I_oC\sqrt{C^2V_d^2}} = \frac{\sqrt{2}(a_2^2r + a_3^2r - a_3E)}{6\sqrt{-I_oC\sqrt{C^2V_d^2}((a_2^2r + a_3^2r - a_3E)}}$$

$a_2 = 0$ and $a_3 - I_d = 0$.

This equations system has two solutions,

$$\left\{a_2 = 0, I_d = \frac{E + \sqrt{E^2 - 8I_0V_dr}}{2r}, a3 = I_d\right\}$$

and $$\left\{a_2 = 0, I_d = \frac{E - \sqrt{E^2 - 8I_0V_dr}}{2r}, a3 = I_d\right\}$$

Then, taking the latter solution, k_1 and the control inputs derived in (4.3) are,

$$k_1 = -\frac{\sqrt{2}\sqrt{I_0^2V_dC\sqrt{2x_1}}}{2I_0C\sqrt{x_1}}$$

$$u1 = -\frac{\omega L(-E + \sqrt{E^2 - 8I_0 v_d r C\sqrt{V_0 V_d}}}{4rV_d}$$

$$u2 = -\frac{E + \sqrt{E^2 - 8I_0 v_d r C\sqrt{V_0 V_d}}}{4V_d}$$

Where, V_0 denotes the output voltage DC component $\langle v_0 \rangle_0$ *and* $\sqrt{2x_1} = \langle q \rangle_0 = C\langle v_0 \rangle_0$

5. SIMULATION RESULTS

The power converter behaviour is simulated using Matlab and Simulink. The following parameters are used for performance analysis of the converter. L = 2mH, C = 1000μF, Load Resistance = 150Ω, V_{in} = 120V, Desired Output DC Voltage = 200 V. Frequency = 50 Hz.

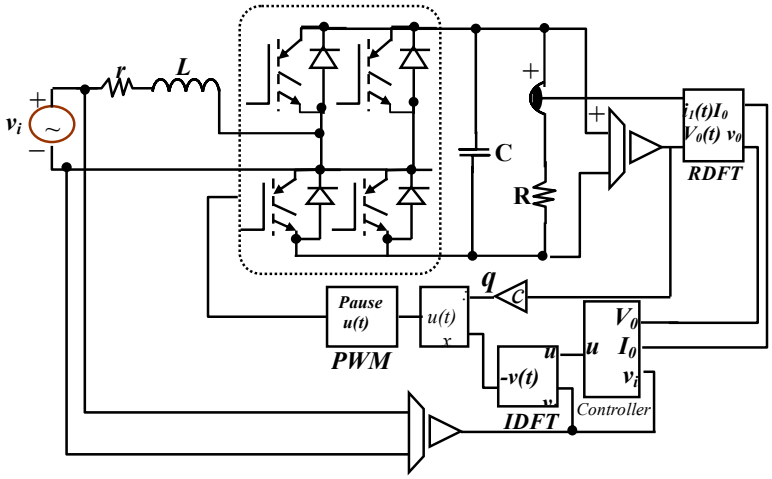

Figure 2 The Structure of the IDA-PB control approach

Figure-2 shows the closed-loop structure of the IDA-PBA control approach. The actual rectifier is shown at the top of the figure with pulses as the input signal and the couple $i_1(t)$ and $v_0(t)$ as the output measured variables. The input voltage $v_i(t)$ is sensed for being used as the input in the controller and the Inverse Discrete Fourier Transform (IDFT) blocks. The Recursive Discrete Fourier Transform (RDFT) allows the right Fourier Coefficients to be obtained at sampling intervals. The controller block computes the suitable averaged Fourier components for the control signal u(t) while the IDFT is performed in the IDFT block to obtain the discrete *v(kT)* control signal.

5.1 Response of uncontrolled and controlled bridge Rectifier

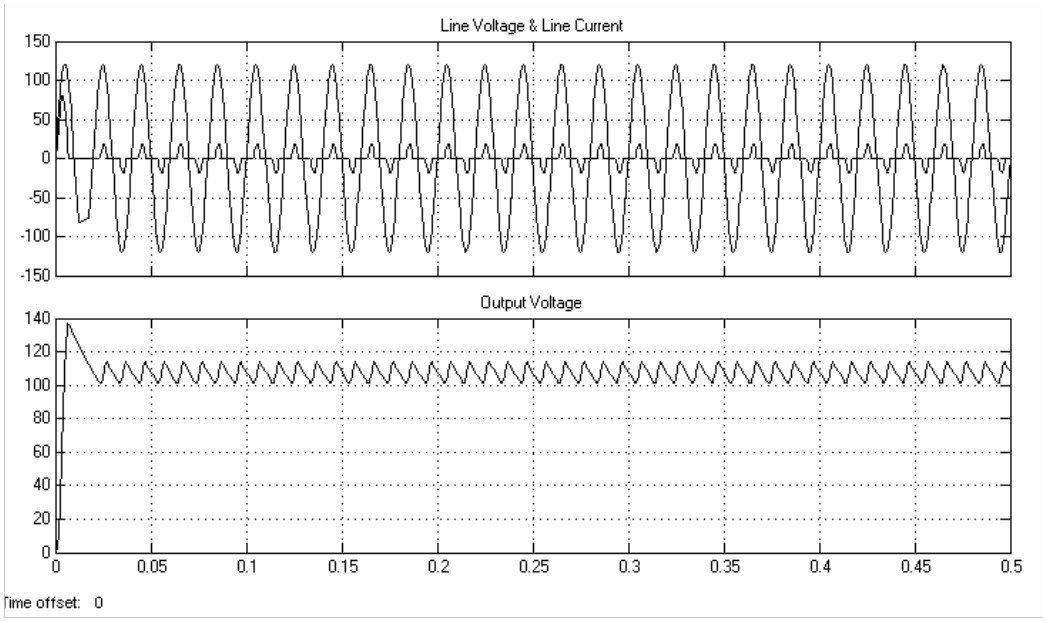

Figure 3. Response of the uncontrolled rectifier

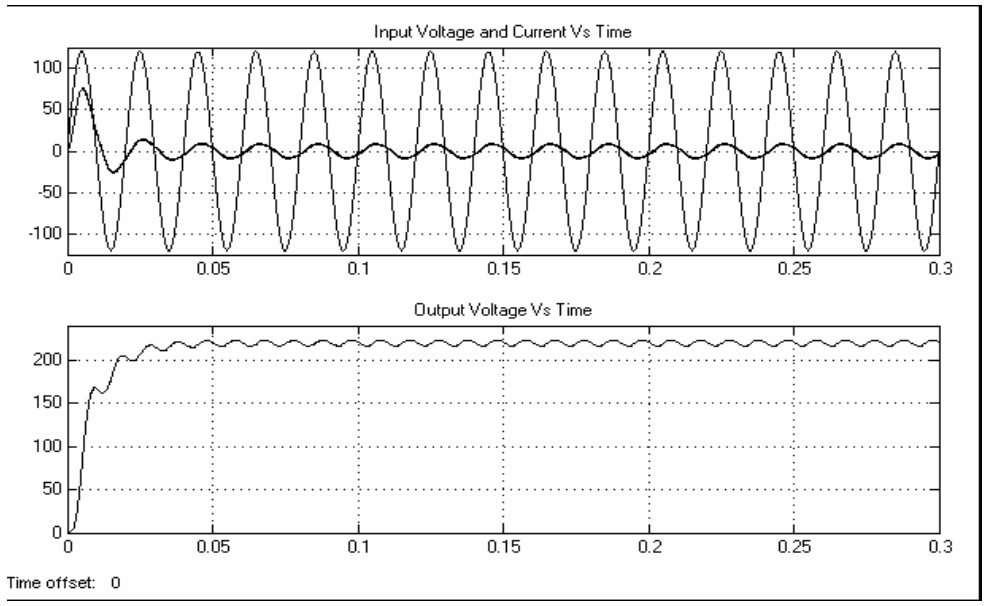

Figure 4. Open Loop Response of controlled bridge rectifier

As seen from the figure 3and 4, the voltage output of the rectifier is less than the desired voltage and also the line current is not exhibiting the sinusoidal waveform. These drawbacks are overcome in the model proposed in this work.

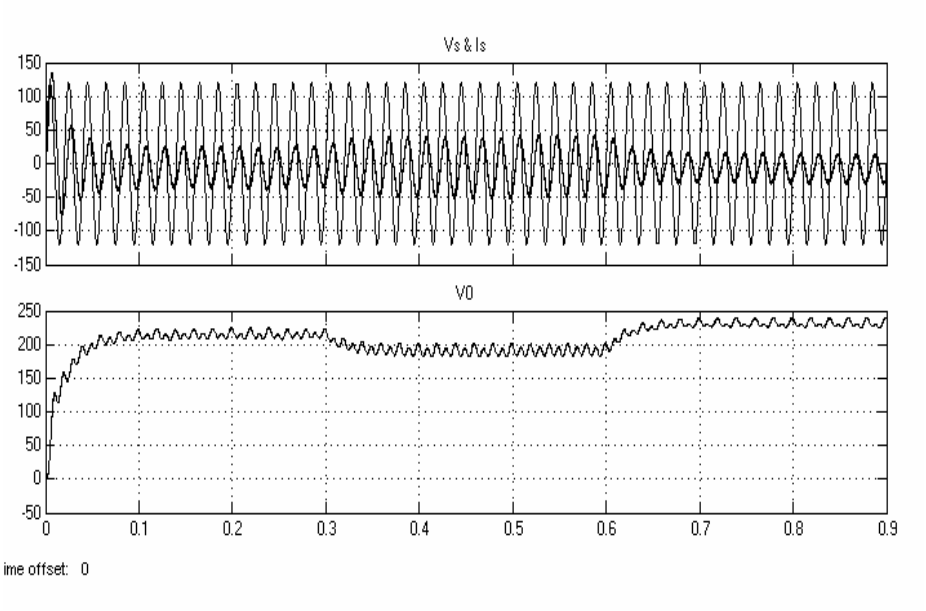

Figure 5 Responses for output voltage and line current

The responses for output voltage and line current waveform in front of load changes are shown in figure 5.

5.2 Responses of Rectifier with Controller Simulink model

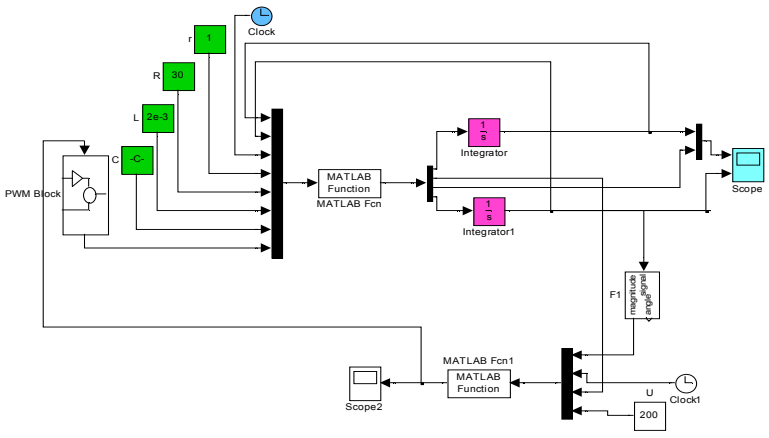

Figure 6. Simulink model of the proposed control scheme.

Figure 6 exhibits the simulink model of the proposed control scheme. Subsequently, figures 7 show the responses of the system in front of load variation. Figure 8 shows the power factor correction performance for the case of nonlinear load which mean value changes from 50 Ω to 500 Ω.

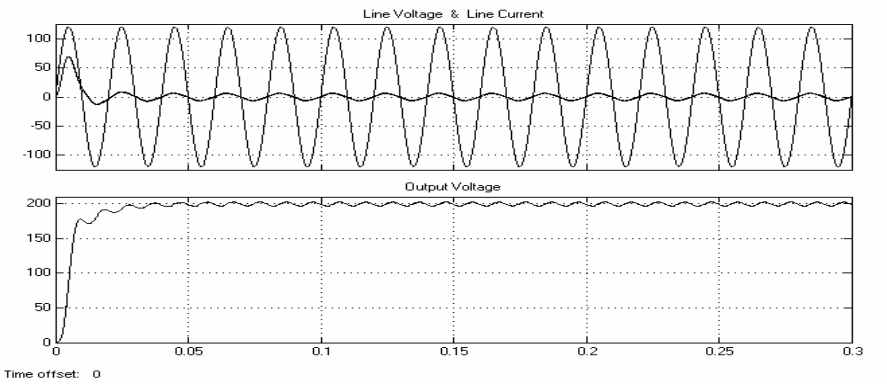

Figure 7 Unity power factor and voltage regulation responses

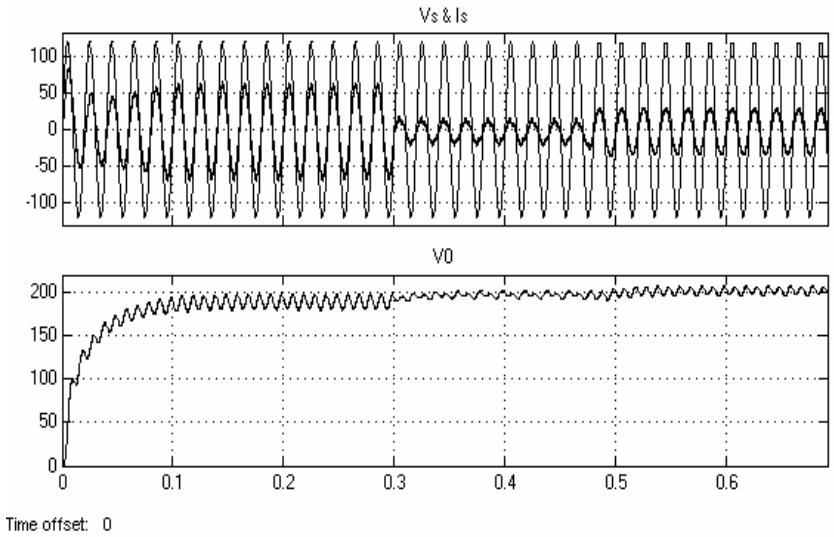

Figure 8 Responses for Vs, Is and Vo which exhibit robustness under load parameter variations (50 Ω to 500 Ω)

The desired regulated DC output voltage and the power factor is V_0 = 200V and near unity respectively. It is important to note that the power losses due to IGBT switches has been taken into account. The system performance could be improved by replacing these IGBT switches with low power ones.

5.3 Comparative discussions of the results

As seen from the figure 2 the line current of ordinary uncontrolled bridge rectifier is not sinusoidal, also there is no boost up of output voltage. However system itself is not robust and also the system power factor is also not unity (figure 3). But from figure 7, it's seen that using the proposed bridge rectifier model it's possible to get a sinusoidal line current and also boost up of output

voltage can also be done. From the figure 7, it's seen that by incorporating the controller it's possible to obtain robustness with respect to load variations and also it's possible to obtain a near unity power factor, figure 8. Initially, the DC bus voltage rests at the diode rectifier level with a resistive load of R = 60 Ω. Then the control action is applied keeping the load resistance and the output voltage increases to the desired DC value. Afterwards two load changes from 50 Ω to 500 Ω were applied and the shape of the DC bus output voltage shows ensures the robustness of the controlled system with respect to load variations.

6. CONCLUSION

The performance analysis of single phase full bridge boost-type rectifier is analyzed for regulated output voltage and unity power factor at the AC mains. In the case considered here, a nonstandard tracking control problem for a full-bridge boost rectifier results in a regulation one because of GSSA expansion for phasor coefficients. An IDA-PB control has been designed measuring the load current and the load voltage, and presuming the input voltage is known. The closed-loop system is robust to load variations achieving unity power factor in the ac mains and load voltage Regulation.

REFERENCES

[1] B. Lin and H. Lu, "Single-phase power-factor-correction ac/dc converters with three pwm control schemes," IEEE Trans. Aerospace. Electron. Syst., vol. 36, no. 1, pp. 189–200, Jan. 2000.

[2] S. Sanders, J. Noworolski, X. Liu, and G. Verghese, "Generalized averaging method for power conversion systems," IEEE Trans. Power Electron., vol. 6, no. 4, pp. 251–259, Apr. 1991.

[3] D. Lee, G. Lee, and K. Lee, "Dc-bus voltage control of three-phase ac/dc pwm converters using feedback linearization," IEEE Trans. Ind. Appl., vol. 36, no. 3, pp. 826–832, May/Jun. 2000.

[4] R. Morici, C. Rossi, and A. Tonielli, "Variable structure controller for ac/dc boost converter," in Proc. IEEE 20th Int. Conf. Industrial Electronics, Control Instrumentation, vol. 3, 1994, pp. 1449–1454.

[5] G. Escobar, D. Chevreau, R. Ortega, and E. Mendes, “An adaptive passivity- based controller for a unity power factor rectifier,” IEEE Trans. Control Syst. Technol., vol. 9, no. 4, pp. 637–644, Jul. 2001.

[6] R. Ortega, A. Schaft, B. Maschke, and G. Escobar, “Interconnection and damping assigment passivity-based control of port-controlled Hamiltonian systems,” Automatica, vol. 38, pp. 585–596, 2002.

[7] J. Mahdavi, A. Emaadi, M. Bellar, and M. Ehsani, “Analysis of power electronic converters using the generalized state-space averaging approach,” IEEE Trans. Circuits Syst. I, vol. 44, no. 8, pp. 767–770, Aug. 1997.

[8] J. Rosendo and A. Gómez, “Efficient moving-window dft algorithms,” IEEE Trans. Circuits Syst. II, Analog Digit. Signal Process. vol. 45, no. 2, pp. 256–260, Feb. 1998.